

THE IMPORTANCE OF LOW LEVEL RANDOM FOR RESONANCE SEARCH IN SPACE MECHANISMS

J. Zemann⁽¹⁾, A. Bolognini⁽¹⁾, S. Battige⁽¹⁾

R. Sgobbo⁽²⁾ and S. Patti⁽³⁾

⁽¹⁾Beyond Gravity AG, Schaffhauserstr. 580, 8052 Zürich (Switzerland), Email: josef.zemann@beyondgravity.com

⁽²⁾Airbus Defence and Space GmbH, Airbus-Allee 1, 28199 Bremen (Germany), Email: riccardo.sgobbo@airbus.com

⁽³⁾European Space Agency, Keplerlaan 1, NL-2200 AG Noordwijk (The Netherlands), Email: sandro.patti@esa.int

ABSTRACT

Design verifications and qualification of space equipment require a passed vibration test.

Low-level sinusoidal (LLS) vibration testing is the state-of-the-art method for equipment integrity, pre-high-level, and post-high-level testing, specifically applied in ESA projects.

This paper studies the effect of using the Low Level Random (LLR) vibration testing method instead of the widely used LLS method.

The presented comparison shows superior results of LLR against LL, studied on the Solar Array Drive Mechanism (SADM) for the European Service Module (ESM) of the Multi-Purpose Crew Vehicle (MPCV) used in the NASA/ESA ARTEMIS Program.

Those results question the common practice of using LLS as the standard method for justification of equipment integrity and in contrast, suggest using LLR instead.

In this common context, our paper demonstrates that LLR outperforms LLS for complex mechanisms.

LLR is more robust than LLS, delivering more consistent results and hence, reduces the chance of misleading results that might be caused by LLS.

1. INTRODUCTION

1.1. MPCV Overview

The Multi-Purpose Crew Vehicle (MPCV) is the spacecraft that NASA intends to use to send humans to lunar orbit and beyond and to return them to Earth. The main purpose is to serve the ARTEMIS program where MPCV is named “Orion” spacecraft. In 2022 the maiden flight successfully took place, and currently nine lunar missions are planned. The MPCV European Service Module (ESM) provides propulsion, cooling, and consumables to the habitable Crew Module (CM). The Solar Array Drive Assembly (SADA) is part of the electrical power generation which is done employing four solar arrays. The Solar Array Drive Mechanisms (SADMs) are the mechanisms, that allow the rotation of the Solar Array Wings (SAWs). They are mounted on the secondary structure of the MPCV-ESM and have mechanical, thermal, and electrical interfaces with the solar arrays and the module.

The mechanism is complex, which poses challenges to characterise the eigenmodes. This paper presents the challenges encountered during the vibration test of the MPCV-ESM3 SADM Flight Model 1 (FM1) and how the Low Level Random (LLR) can effectively be used as an alternative to Low Level Sine (LLS) during resonance search for space mechanisms.

1.2. SEPTA60 Main Components

For decades, Beyond Gravity (formerly RUAG Space) provides the international space market with a series of high-quality Solar Array Drive Mechanisms like SEPTA33, SEPTA36, SEPTA25,... None of these fulfilled the needs for MPCV so a dedicated Solar Array Drive Mechanism “SEPTA60” was developed based on existing heritage. In typical missions, after deployment of the Solar Array Wings (SAW), the loads on the SADM are moderate.

In the Artemis mission, in contradiction, massive boost manoeuvres like Trans Lunar Injection (TLI) cause heavy bending loads. To reduce the bending loads and as well to protect the SAW from boost plume a dedicated second axis is introduced to allow tilting.



Figure 1: SAW Position

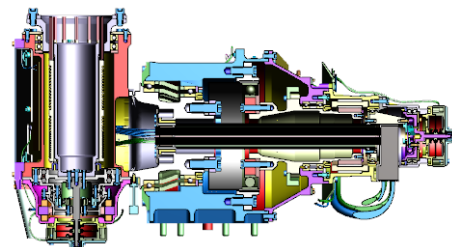


Figure 2: SEPTA 60

The outer axis (Figure 2 left) can be regarded as a standard Solar Array Drive Mechanism allowing continuous rotation. Electrical power and Signals from the SAW are transferred by slip rings. A stepper motor is connected to the main axis by a Harmonic Drive (HD) mechanism.

Since the inner axis (Figure 2 right) has to transfer massive boost loads to the spacecraft (S/C), strong bearings are needed. A stepper motor is connected by a harmonic drive to the main axis. For some manoeuvres, the induced torsional load (>1000 Nm) is too high that it can be held by the actuator system. So, a dedicated mechanical brake is implemented which is disengaged during launch by a launch lock as the SAW are fixed by a dedicated hold-down mechanism.

As the inner axis performs only tilting motions the electrical power and signals are transferred to the S/C by a Twist Cartridge.

To serve all challenging mechanical and structural requirements the mechanism consists of 15 rows of ball bearings and 5 sliding/tribological interfaces (e.g. harmonic drive, gear)

2. INITIAL TEST CAMPAIGN

2.1. SEPTA60 Test Flow

The MPCV-ESM SADM is a critical mechanism for the mission and as such is submitted to a very detailed acceptance testing campaign whose flow is reported in, Figure 3. The campaign includes both axis level tests performed independently on the Inner Axis (IA) and Outer Axis (OA), and SADM level tests. After the initial Continuity and Insolation (C&I) test and fine potentiometer adjustment, the IA and the OA are submitted to Thermal Vacuum (TV) test. In addition to that, the IA has to undergo the holding torque test before the two axes are mated and the SADM level test can start. The C&I is then repeated plus the physical properties, grounding, bonding, and functionalities are verified prior to vibration testing. This provides a clear status of the mechanism's health before initiating the vibration test, which is affecting the fatigue damage.

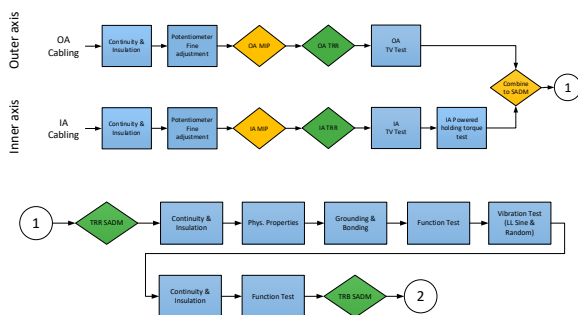


Figure 3: Test Flow

2.2. SEPTA60 ESM3 FM1 Initial Vibration Test

The vibration test flow, reported in Figure 4, is well-established. A dry run is performed on the vibration adapter after every axis reconfiguration, each axis is tested independently, the full level random is preceded by -3 dB and -6 dB runs and LLS are used to identify and compare the eigenmodes before and after every random test. Twelve accelerometers are installed on the unit to monitor the modal behaviour, The most relevant for this work are the ones on the OA and in particular the SAW Interface (IF) and the OA Potentiometer, see Figure 5. During the MPCV-ESM3 SADM FM1 vibration test campaign an unexpected phenomenon was observed. After the application of the first High Level Random (HLR) -6 dB run on the X-axis, the frequency of a main mode shifted by ~23 %, thus being a major concern for structural integrity and violating the ECSS requirements of ± 5 % of max frequency shift between pre-vs-post resonance search. Interestingly, after pausing the test overnight, and performing another LLS in the morning, the eigenfrequency when back to its original frequency. of ~273 Hz. At this point, another application of HLR -6 dB was performed and then a frequency shift of only 9.5% was observed. The resonance searches were performed with LLS and the Frequency Response Functions (FRF) of the OA Potentiometer are reported in Figure 6 where: xLLS_1 curve is the initial one, xLLS_2 is right after HLR -6 dB, xLLS_3 is after overnight rest in a thermally controlled environment and xLLS_4 is after the second application of HLR -6 dB.

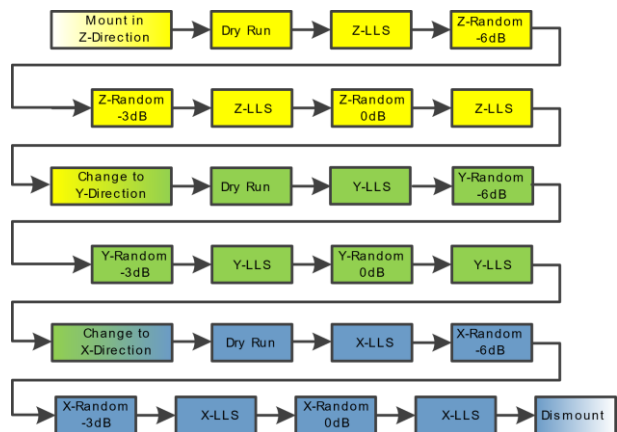


Figure 4: Vibration Test Flow

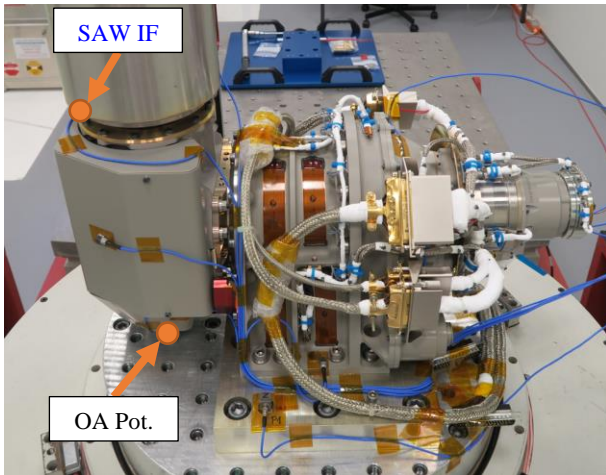


Figure 5: Vibration Test Setup for Z direction: MPCV-ESM3 SADM FM

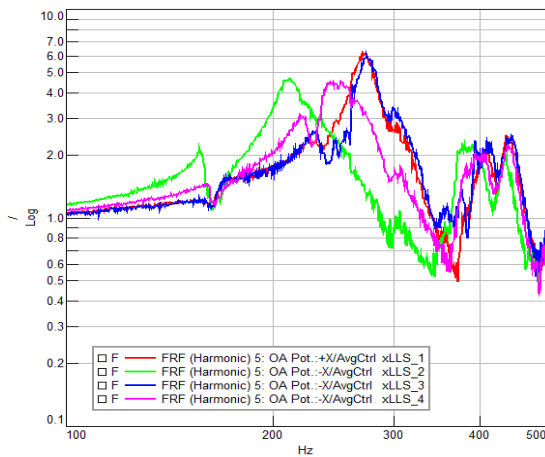


Figure 6: FRFs for OA Potentiometer measured with LLS during MPCV-ESM3 SADM FM1 testing on X axis

3. INVESTIGATION

3.1. SEPTA60 Investigation

The measured frequency shifts observed both on X- and Z-axis, the one on X-axis being the most prominent, were compared to the other SEPTA models and considered out of the family. Raising major concerns, additional hardware and analysis investigations have been agreed during the Non-conformance Review Board (NRB).

Review of the assembly procedures/photographs, X-Ray inspection, and review of component test results, in particular ball bearing preload, were required for the former, while transfer function sensitivity analysis on ball bearing and Harmonic Drive (HD) stiffness were required for the latter. The hardware related investigations did not provide any clear sign of errors: the workmanship was good and the X-Ray inspection confirmed that every component was properly assembled and in good shape.

Moreover, according to the analysis, such a significant frequency shift could only be explained by a change of about 50 % in the bearing stiffness. Nonetheless, this was considered unlikely and additional analysis with PRIMODAL software was performed to identify and compare the modal parameters of each test. In the same timeframe the data acquired during vibration tests were processed once more to look for some other evidence of the mechanism's health.

During the investigation, the FRF acquired during the HLR were compared and it was observed that the modal behaviour of the unit, when subjected to random, was much closer to the FRF measured with LLS right after the first HLR -6 dB application. This is well visible by comparing the xLLS_2 FRF of Figure 6, where the first relevant mode is at 210 Hz, with both xRND_-6dB_1 and xRND_-6dB_2 of Figure 7 where the first mode is at ~215 Hz. Moreover, this test series was repeated twice, and the results are well aligned meaning there's no sign of a possible damage caused by the random vibration.

Please note that the ditches present in the FRF acquired during random are due to a bug in the shaker control software: reprocessing of the data proved that as it is visible in Figure 8.

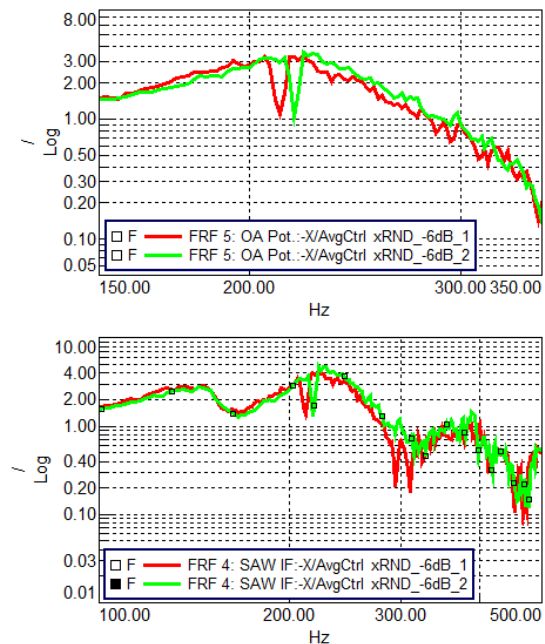


Figure 7: FRFs for OA Potentiometer measured with HLR during MPCV-ESM3 SADM FM1 testing on X-axis

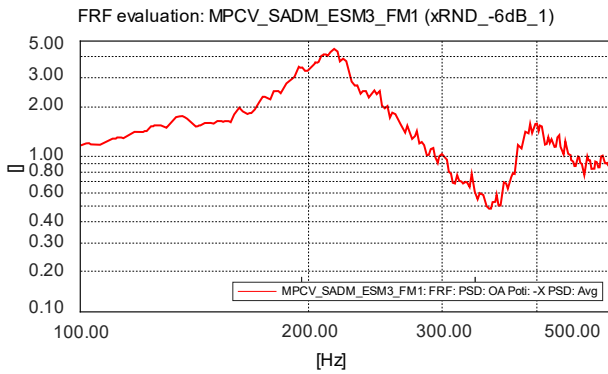


Figure 8: FRFs for OA Potentiometer during MPCV-ESM3 SADM FM1 testing on X axis: data reprocessing

3.2. PRIMODAL Analysis

PRIMODAL is a software tool for the analysis, improvement and especially for the understanding of a structure's dynamic behaviour. Among other capabilities, PRIMODAL can be used to compare test data and simulation data with one another. In addition, the eigenmodes and the behaviour of these modes from vibration tests can be visualized. This function was used in this paper.

The first peak shows a strong frequency shift after the first random event (based on the LLS FRF) but recovers during the night (red line in Figure 6). After the RND FRF it is very stable. More detailed analysis of the mode shapes between ESM3-FM1-xLLS2 (green) and ESM3-FM-xLLS2 (blue) in Figure 6 is performed.

By comparing the mode shape of the first (about 200Hz) and the second (about 270Hz) peak between LLS runs, the mode shapes match the motion remarkably well, although the deflections are not identical.

The Mac-Values and mode shape comparison further strengthens the assumption that these are the same modes. The amplitudes differ and therefore assume different damping rates.

The first peak has the following behaviour (around 200Hz):

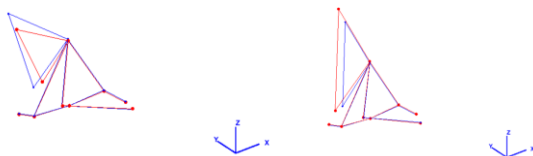


Figure 9: First Eigenmode shapes (around 200Hz) of ESM3-FM1-xLLS2 and ESM3-FM-xLLS2

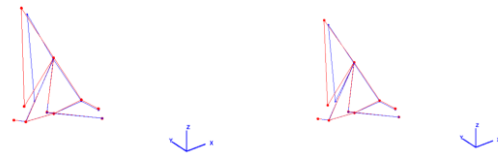


Figure 10: Second Eigenmode shapes (around 273Hz) of ESM3-FM1-xLLS2 and ESM3-FM-xLLS2

Mode 275 Hz for LL3 has much lower amplitude wrt. LL2 (no peak), but the component behaviour is identical at this position. Therefore, the assumption is that this mode was simply heavily damped, but not shifted.

3.3. Preliminary Conclusion and Way Forward

The PRIMODAL study, which pointed towards an abrupt change in damping rather than a frequency shift of the mode as initially supposed, in combination with other supporting evidence (functional and performance testing, X-ray, FRF acquired during random, etc.), allowed for the MPCV-ESM3 SADM FM1 to be judged as healthy. The only open point in the root cause analysis is the non-linear effects. The observed differences can be assimilated to non-linear slip-stick effects which might be thermally or mechanically activated: in fact, as discussed in §2.2, and §3.1, the FRFs acquired during random are very stable and xLLS_3 was in line with xLLS_1 after a long rest time where no activities have been performed on the mechanism in a thermally controlled environment.

It was therefore agreed, during the NRB process, to continue the vibration test but, unfortunately, the IA was disconnected from the OA to perform the X-ray inspection and because of that the acceptance vibration test had to be repeated on every axis. In addition to that it was agreed to perform a survey to identify a better input level for the LLS and to perform additional LLR FRF after every HLR to have a more complete picture.

3.4. Fracture Control Analysis

The additional tests that were agreed during the NRB and due to the fact that the IA and OA were uncoupled required that the fracture control analysis consider these additional load cycles.

With the planned test changes, the fracture control and thus the lifetime analysis of the mechanism was also considered. In the process, particular attention was paid to the following points.

The starting point was that the random load set covers two sets of acceptance tests, so the margin and one repetition are considered already. This set is multiplied by three. That is a total of six sets of acceptance test covered.

Location	Initial flaw size	a/c	Load Block	# Lifes	Cracksize end of life		Crack Status
					a [mm]	c [mm]	
Rear Rib	Eddy current - 1.905	1.0	1-31, 32-37	4	3.158	3.324	Critical Crack Size has NOT been reached.
Actuator Bearing I/F		1.0	1-31, 32-37	4	6.268	6.478	

Increased random vibration duration (factor:3)

Location	Initial flaw size	a/c	Load Block	# Lifes	Cracksize end of life		Crack Status
					a [mm]	c [mm]	
Rear Rib	Eddy current - 1.905	1.0	1-31, 32-37	4	3.807	4.040	Critical Crack Size has NOT been reached.
Actuator Bearing I/F		1.0	1-31, 32-37	3.987	-	6.851	

Rear rib and Actuator bearing achieve the lifetime requirement of 4 cycles. Max achievable life for both locations is approximately 4. Increased random vibration duration (factor:3) plus LLS at 1.2 g with reduced conservatism.

Location	Initial flaw size	a/c	Load Block	# Lifes	Cracksize end of life		Crack Status
					a [mm]	c [mm]	
Rear Rib	Eddy current - 1.905	1.0	1-31, 32-37	4	3.926	4.170	Critical Crack Size has NOT been reached.
Actuator Bearing I/F		1.0	1-31, 32-37	4	4.769	5.712	

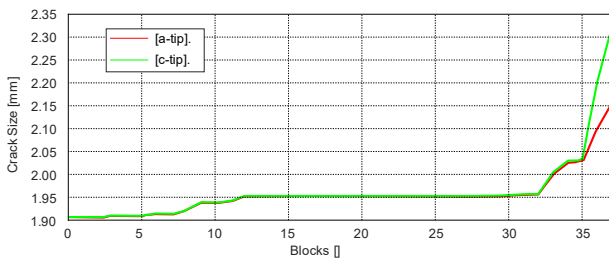


Figure 11: Crack Growth Results

The increase in the duration of the random vibration and the LLS do not cause any lifetime issues in these locations. The fracture control analysis shows that the modified test has a negligible effect on the lifetime of the mechanism.

4. FINAL TEST CAMPAIGN

4.1. SEPTA60 ESM3 FM1 final vibration test flow

As discussed in §3.3 it was agreed to include LLR, which corresponds to HRL -9 dB, before and after every HLR run resulting in the following test sequence for each axis:

- LLS
- RND -9dB, RND -6dB, RND -9dB (Note, is tested in one run)
- LLS
- RND -9dB, -3dB, RND -9dB (Note, is tested in one run)
- LLS
- RND -9dB, 0dB, RND -9dB (Note, is tested in one run)
- LLS

For the first axis also an additional sine level survey was carried out with the aim to identify a more suitable level

for the sine vibration which could possibly lead to more consistent results. The final test flow for the X-axis, compared to a nominal flow, is reported in Figure 12.

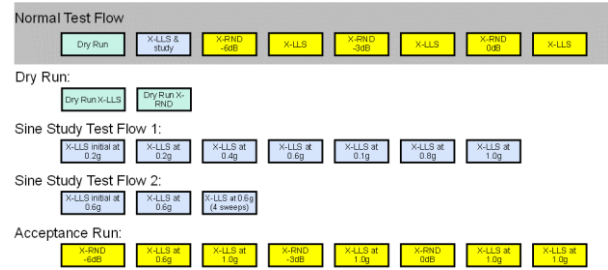


Figure 12: MPCV-ESM3 SADM FM1 vibration re-test flow

4.2. SEPTA60 ESM3 FM1 final vibration test LLS survey

Several Low-Level Sines with different amplitudes before the HLR have been performed during the first two days. The curves, reported in Figure 13 are in order of execution and it is clearly visible that the response is input dependent: the lower the input the higher the peak frequency. In fact, the first peak in the spectra is at 199Hz when probed at 1 g input, while it shifts to 249Hz when 0.1g is used as input. During the second day additional LLS runs have been performed in sequence to check for variation of the response with the same input which was set to 0.6 g for this trial: the results are reported in Figure 14.. The plots are reported in order of execution and there is a clear dependency of the results with respect to the execution time. This is again a confirmation that there are non-linear effects that results in very different frequency response.

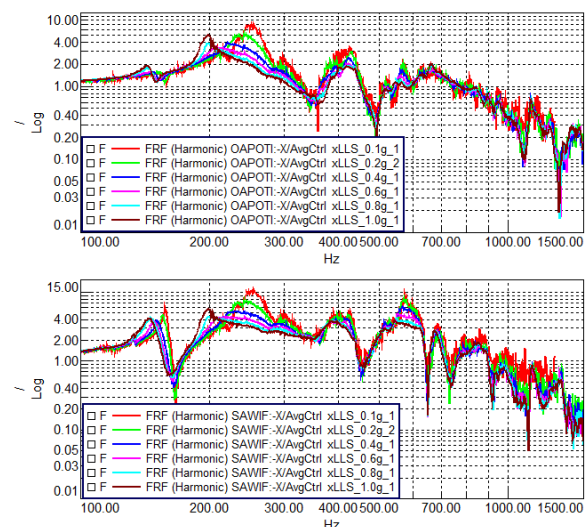


Figure 13: FRFs for OA Potentiometer and SAWIF measured with LLS during MPCV-ESM3 SADM FM1 re-testing: sine survey.

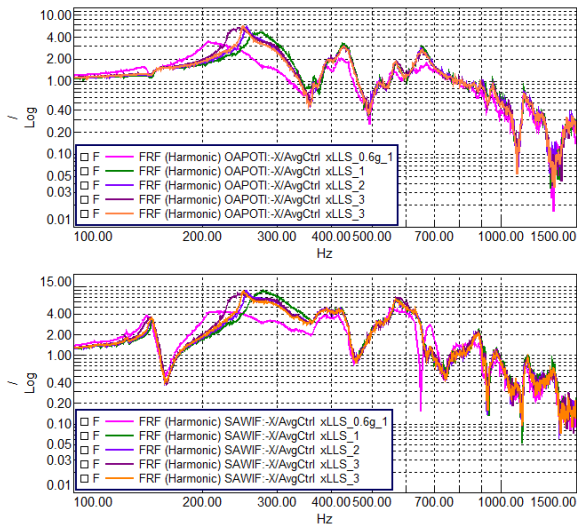


Figure 14: FRFs for OA Potentiometer and SAW IF measured with LLS during MPCV-ESM3 SADM FM1 re-testing: sinusoidal sweep at 0.6

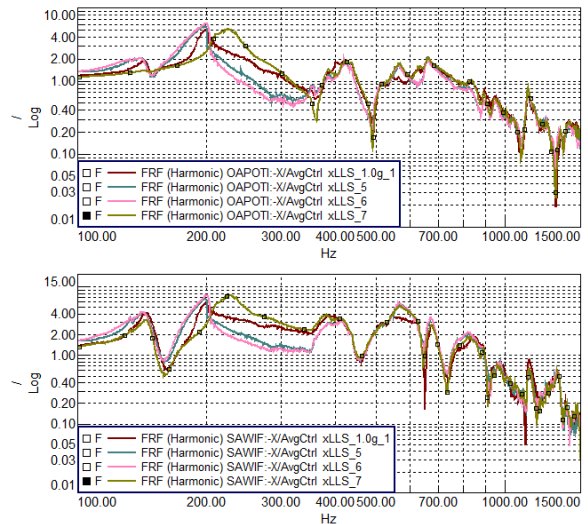


Figure 15: OA Potentiometer FRFs comparison between LLS and LLR; MPCV-ESM3 SADM FM1 re-testing

4.3. SEPTA60 ESM3 FM1 final vibration test LLR

The HLR was then performed by following the flow presented in §4.1; the results are reported in Figure 15. The reported plots are on top for LLS and on the bottom for LLR (HLR -9 dB) performed in this sequence: before HLR -6 dB, after HLR -6 dB, after HLR -3 dB and after HLR 0dB. As it is possible to see, the frequency shift recorded with LLS is greater than the one measured with LLR: 13.5 % and 7.9 % respectively. An additional comparison was performed between LLR. The results are reported in Figure 16, where: on top only the FRF acquired during LLR (full level LLR -9 dB) before -6 dB, -3 dB and 0 dB runs, while on the bottom plot the ones acquired after -6 dB, -3 dB and 0 dB runs.

This makes it even more clear that the non-linearity in the unit is thermally driven. There is no difference in the FRFs acquired during LLR before the HLR and the only difference with those acquired right after the HLR is the dwell time in between runs.

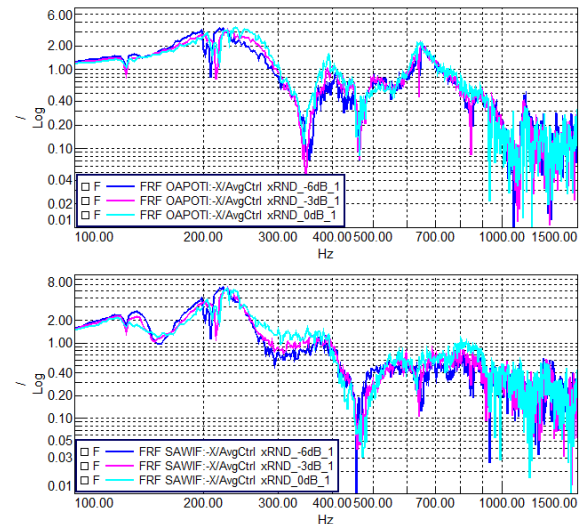


Figure 16: OA Potentiometer FRFs comparison between LLR; MPCV-ESM3 SADM FM1 re-testing.

5. CONCLUSION

The Low Level Sine (LLS) comparison proved to be an unreliable method to detect the eigenmodes for MPCV-ESM3 SADM FM1, due to non-linearities, friction and backlash, which influence the operating conditions of the system, resulting in misinterpretation of the health status; a similar behaviour has been noticed also on different mechanisms at Beyond Gravity (former RUAG Space Switzerland).

FRFs acquired during Low Level Random (LLR), instead, proved to be very consistent while also providing more accurate values for the structural damping since the input level and also the type of input are much closer to the actual vibration environment at launch. The usage of the LLR for resonance search is already considered in the ECSS-E-ST-10-03C for acoustic testing: “A low-level

acoustic run (-8 dB the qualification level) shall be performed before and after the acoustic qualification run by determining resonant frequencies". The experience with MPCV-ESM SADM proved that the LLR can be effectively used on space mechanism, and it is indeed highly recommended to follow the LLR-based vibration test flow, reported in §4.1, especially for complex mechanisms which can present non-linear behaviour.

6. REFERENCES

1. ARTEMIS Plan; NASA's Lunar Exploration Program Overview September 2020 NP-2020-05-2853-HQ
2. NASA Orion Space Craft
617409main_orion_overview_fs_33012.pdf
3. ESA ORION ESM overview WebPage:
https://www.esa.int/Science_Exploration/Human_and_Robotic_Exploration/Orion/European_Service_Module
4. Primodal Support <https://primodal.com/>